Monthly Notices of the ROYAL ASTRONOMICAL SOCIETY

MNRAS **529,** 4554–4564 (2024) https://doi.org/10.1093/mnras/stae815
Advance Access publication 2024 March 20

Formation of lower mass-gap black hole–neutron star binary mergers through super-Eddington stable mass transfer

Jin-Ping Zhu [1,2★] Ying Qin [3★] Zhen-Han-Tao Wang [4] Rui-Chong Hu [5] Bing Zhang [5,6] and Shichao Wu [7,8]

[1]*School of Physics and Astronomy, Monash University, Clayton, VIC 3800, Australia*
[2]*OzGrav: The ARC Centre of Excellence for Gravitational Wave Discovery, Calyton, VIC 3800, Australia*
[3]*Department of Physics, Anhui Normal University, Wuhu, Anhui 241002, China*
[4]*Guangxi Key Laboratory for Relativistic Astrophysics, School of Physical Science and Technology, Guangxi University, Nanning 530004, China*
[5]*Department of Physics and Astronomy, University of Nevada, Las Vegas, NV 89154, USA*
[6]*Nevada Center for Astrophysics, University of Nevada, Las Vegas, NV 89154, USA*
[7]*Max-Planck-Institut für Gravitationsphysik (Albert-Einstein-Institut), D-30167 Hannover, Germany*
[8]*Leibniz Universität Hannover, D-30167 Hannover, Germany*

Accepted 2024 March 15. Received 2024 February 25; in original form 2023 September 29

ABSTRACT

Super-Eddington accretion of neutron stars (NSs) has been suggested both observationally and theoretically. In this paper, we propose that NSs in close-orbit binary systems with companions of helium (He) stars, most of which systems form after the common-envelope phase, could experience super-Eddington stable Case BB/BC mass transfer (MT), and can sometimes undergo accretion-induced collapse (AIC), resulting in the formation of lower mass-gap black holes (mgBHs). Our detailed binary evolution simulations reveal that AIC events tend to happen if the primary NSs have an initial mass $\gtrsim$1.7 $M_\odot$ with a critical accretion rate of $\gtrsim$300 times the Eddington limit. These mgBHs would have a mass nearly equal to or slightly higher than the NS maximum mass. The remnant mgBH–NS binaries after the core collapses of He stars are potential progenitors of gravitational-wave (GW) sources. Multimessenger observations between GW and kilonova signals from a population of high-mass binary NS and mgBH–NS mergers formed through super-Eddington stable MT are helpful in constraining the maximum mass and equation of state of NSs.

Key words: gravitational waves – binaries: general – stars: Wolf–Rayet – black hole–neutron star mergers.

1 INTRODUCTION

On the one hand, the X-ray and radio observations of Galactic pulsars revealed a likely neutron star (NS) maximum mass of ∼2–2.3 $M_\odot$ (e.g. Antoniadis et al. 2013; Alsing, Silva & Berti 2018; Romani et al. 2022), consistent with the maximum mass inferred by the observations of NSs in gravitational-wave (GW) binaries (e.g. Margalit & Metzger 2017; Landry & Read 2021; Zhu et al. 2022a; Abbott et al. 2023a). On the other hand, the measurements of the mass distribution of black holes (BHs) in Galactic X-ray binaries suggested a lower boundary close to ∼5 $M_\odot$ (Bailyn et al. 1998; Özel et al. 2010; Farr et al. 2011). This led to the conjecture of the presence of the mass gap between the heaviest NSs and lightest BHs, which was thought to be potentially caused by the observational bias (Kreidberg et al. 2012), natal kick (Mandel et al. 2021), or the intrinsic physics mechanism of core-collapse supernova (SN) explosions, e.g. the rapid model (Fryer et al. 2012). However, recent electromagnetic (EM) observations discovered a few compact objects with mass plausibly lying in the range of ∼2.5–5 $M_\odot$, indicating that the putative mass gap could be at least partly populated. For example, gravitational microlensing identified eight compact-object candidates with masses within the mass gap (Wyrzykowski & Mandel 2020). Thompson et al. (2019) reported that the unseen companion of giant star 2MASS J05215658+4359220 could have a mass of $3.3^{+2.8}_{-0.7}$ $M_\odot$, which could be a non-interacting mass-gap black hole (mgBH). Using radial velocity measurements, Rivinius et al. (2020) suggested HR 6819, a star in a hierarchical triple system, might be accompanied by an unseen companion, which could be a non-accreting BH with a mass of ≥4.2 $M_\odot$. van der Meij et al. (2021) calculated a mass of 4U 1700−37 of 2.54 $M_\odot$, which could be either an NS or a BH in the mass gap. Andrews, Taggart & Foley (2022) used *Gaia* data release to estimate the masses of the dark companions in wide-orbit binaries, which span a range of 1.35–2.7 $M_\odot$, partially intersecting with the mass gap.

Currently, it remains uncertain that whether X-ray binaries and GW sources follow a similar evolutionary pathway (e.g. Belczynski et al. 2021; Fishbach & Kalogera 2022). It is also expected that GW searches could discover a number of mgBHs in the merging systems of binary BH–NS and binary BH (BBH). During the third observing run (O3) of the LIGO–Virgo–KAGRA (LVK) Collabo-

★ E-mail: jin-ping.zhu@monash.edu (J-PZ); yingqin2013@hotmail.com (YQ)

ration, a few GW candidates that potentially contain a mass-gap compact object were indeed detected. GW190814 was reported to be a merger between a $23.2^{+1.1}_{-1.0}\,M_\odot$ BH and a mass-gap compact object with a mass of $2.59^{+0.08}_{-0.09}\,M_\odot$ (Abbott et al. 2020b). The LVK Collaboration also detected a similar, but marginal event, namely GW200210_092254 in O3 (Abbott et al. 2023b), where the component masses were inferred to be $24.1^{+7.5}_{-4.6}$ and $2.83^{+0.47}_{-0.42}\,M_\odot$, respectively. The posterior distributions for the primary source mass of the low-significance BH–NS candidate GW190426_152155 and the BH–NS merger GW200115, i.e. $5.7^{+3.9}_{-2.3}$ and $5.9^{+1.4}_{-2.1}\,M_\odot$, partly lie in the mass gap (Abbott et al. 2021a, b). However, by applying alternative astrophysically motivated priors, the primary mass of GW200115 would be more tightly constrained to be $7.0^{+0.4}_{-0.4}\,M_\odot$ (Mandel & Smith 2021), which could be completely higher than the mass gap. Furthermore, the secondary component of GW191113_071753 has a mass of $5.9^{+4.4}_{-1.3}\,M_\odot$ with 13 per cent probability of being an mgBH (Abbott et al. 2023b). Despite the detection of a few GW candidates containing mass-gap compact objects in O3, the population properties of merging compact binaries using GWs in the Gravitational-Wave Transient Catalog 2 (GWTC-2) and the Gravitational-Wave Transient Catalog 3 (GWTC-3) still indicated a relative dearth of events with masses in the mass gap (Farah et al. 2022; Olejak et al. 2022; van Son et al. 2022; Ye & Fishbach 2022; Zhu et al. 2022a; Abbott et al. 2023a; Biscoveanu, Landry & Vitale 2023).

Systematic investigations of BH–NS systems formed through isolated binary evolution have been recently explored (e.g. Román-Garza et al. 2021; Hu et al. 2022; Xing et al. 2023; Wang et al. 2024). Binary population synthesis showed that the rapid SN model does not form any mgBHs (e.g. Belczynski et al. 2012; Giacobbo & Mapelli 2018), while the delayed and stochastic models (Mandel & Müller 2020) suggested that ∼30–80 per cent of BH–NS mergers and ∼20–40 per cent of BBH mergers are expected to host at least one mgBH (e.g. Shao & Li 2021; Drozda et al. 2022). Both scenarios appear to be inconsistent with the observational results from GWTC-3. On the other hand, NSs can undergo accretion-induced collapse (AIC) to mgBHs via accretion when NSs grow to the point of exceeding the maximum mass allowed by their equation of state (EoS). AICs of accreting NSs are mostly predicted to take place in intermediate/low-mass X-ray binaries with companions of degenerated hydrogen/He dwarf stars (MacFadyen, Ramirez-Ruiz & Zhang 2005; Dermer & Atoyan 2006; Giacomazzo & Perna 2012; Gao, Li & Shao 2022; Chen et al. 2023). Furthermore, based on the standard scenario of the formation of a binary NS (BNS) system (e.g. Bhattacharya & van den Heuvel 1991; Tauris et al. 2017; Vigna-Gómez et al. 2018), an NS orbiting a main-sequence star needs to undergo common-envelope phase to become a close-orbit NS–He star system when the secondary star expands to a giant star. The NS could accrete materials from the hydrogen envelope during the common-envelope phase and from the He star during the subsequent Case BB/BC mass transfer (MT) phase to increase its mass. As predicted by several simulations (e.g. MacLeod & Ramirez-Ruiz 2015; Esteban, Beacom & Kopp 2023), since the common-envelope stages are months long with accretion rates up to $\dot{M} \lesssim 0.1\,M_\odot$ if the super-Eddington accretion for the NS is permissible, the MT during the common-envelope phase is usually limited during this phase. The discovery that a number of ultraluminous X-ray sources (ULXs) are pulsating NSs unambiguously suggested that a fraction of NSs in binary systems can accrete at a super-Eddington accretion rate (see Kaaret, Feng & Roberts 2017, for a review). Population synthesis simulations by Shao, Li & Dai (2019) suggested that a significant fraction of NS ULXs in a Milky Way-like galaxy could contain a He star companion. Most recently, Zhou, Feng & Bian (2023) for the first time identified a He donor star in NGC 247 ULX-1. Thus, some NSs could experience super-Eddington accretion in an NS–He star binary during the stable MT stage. The MT rates could range from a few 10^{-5} to a few $10^{-4}\,M_\odot\,\mathrm{yr}^{-1}$ with durations of a few 10^4 yr. Thus, AIC of an NS to an mgBH could happen if the NS reaches its maximum mass after accreting sufficient materials. In this paper, we present a new formation scenario in which an accreting NS during the stable Case BB/BC MT with super-Eddington accretion could undergo AIC leading to the formation of an mgBH. The final remnant system could be an ideal GW source of an mgBH–NS binary merger if the binary system survives the second SN.

2 MODELLING

2.1 Super-Eddington accretion of NSs

Traditionally, the accretion rate of compact objects is thought to be limited by the Eddington limit, i.e.

$$\dot{M}_{\rm Edd} = \frac{4\pi G M_{\rm acc}}{\kappa c \eta} = 3.6\times10^{-8}\left(\frac{M_{\rm acc}}{1.4\,M_\odot}\right)\kappa_{-0.47}^{-1}\eta_{-1}^{-1}\,M_\odot\,\mathrm{yr}^{-1}, \quad (1)$$

with the Eddington luminosity of

$$L_{\rm Edd} = \eta\dot{M}_{\rm Edd}c^2 = \frac{4\pi G M_{\rm acc} c}{\kappa} = 2.1\times10^{38}\left(\frac{M_{\rm acc}}{1.4\,M_\odot}\right)\kappa_{-0.47}^{-1}\,\mathrm{erg\,s^{-1}}, \quad (2)$$

where $M_{\rm acc}$ is the accretor's mass, κ is the opacity of the accreting material, G is the gravitational constant, and c is the speed of light. Hereafter, the conventional notation $Q_x = Q/10^x$ is adopted in cgs units. The radiation efficiency of accretion η is set to be $\eta = 0.1$ for an NS accretor and $\eta = 1-\sqrt{1-(M_{\rm BH}/M_{\rm BH,i})^2/9}$ if $M_{\rm BH} < \sqrt{6}M_{\rm BH,i}$ for a BH accretor (Podsiadlowski, Rappaport & Han 2003), where $M_{\rm BH}$ is the BH mass and $M_{\rm BH,i}$ is the initial BH mass that is equal to the NS maximum mass $M_{\rm NS,max}$. In our work, $M_{\rm NS,max} \sim 2.2\,M_\odot$ is defined following the constraints by the observations of Galactic pulsars and GW binaries (e.g. Margalit & Metzger 2017; Romani et al. 2022; Zhu et al. 2022a; Abbott et al. 2023).

The discoveries of NS ULXs demonstrated that NSs can accrete at a super-Eddington rate. Some of ULXs, e.g. M82 X-2 (Bachetti et al. 2014), NGC 7793 P13 (Fürst et al. 2016), and NGC 1313 X-2 (Sathyaprakash et al. 2019), have an apparent luminosity of a few $10^{40}\,\mathrm{erg\,s^{-1}}$ implying that the accretion rate could be $\gtrsim 100\,\dot{M}_{\rm Edd}$. Israel et al. (2017) reported that NGC 5907 ULX-1 and some other extreme ULXs that might harbour NSs can even have a maximum X-ray luminosity of a few $10^{41}\,\mathrm{erg\,s^{-1}}$ corresponding to $\sim 1000\,\dot{M}_{\rm Edd}$ if the emission is isotropic.

For a standard gas-pressure-dominated thin disc with super-Eddington accretion, the location at which the accretion disc just possesses a local luminosity reaching the Eddington limit and has mass loss is defined as the spherization radius (Shakura & Sunyaev 1973), i.e.

$$R_{\rm sph} \approx \frac{3\kappa\dot{M}}{8\pi c}, \quad (3)$$

where $\dot{M}$ is the accretion rate of the disc. Furthermore, the NS magnetic field can interact with the accretion disc. The disc around a magnetized NS is disrupted at the magnetospheric radius (Frank,

King & Raine 2002), which is given by

$$R_{\rm mag} = \xi R_{\rm A} = \xi \left(\frac{\mu^2}{\dot{M}_{\rm in}\sqrt{2GM_{\rm NS}}} \right)^{2/7}, \quad (4)$$

where $R_{\rm A}$ is the Alfvén radius, ξ is the dimensionless coefficient (Ghosh & Lamb 1979; Wang 1996; Long, Romanova & Lovelace 2005; Kulkarni & Romanova 2013), $\dot{M}_{\rm in}$ is the accretion rate at $R_{\rm mag}$, $M_{\rm NS}$ is the NS mass, and $\mu = B_{\rm NS}R_{\rm NS}^3$ is the magnetic moment of the NS with $B_{\rm NS}$ and $R_{\rm NS}$ being the magnetic field strength and radius of the NS, respectively. One can determine a critical accretion rate of $\dot{M}_{\rm cr} \propto \mu^{4/9}$, which provides a limit on $\dot{M}_{\rm in}$ by equating $R_{\rm mag}$ with $R_{\rm sph}$. Thus, the NS accretion with a higher super-Eddington critical rate requires a larger NS magnetic field. If $R_{\rm mag} \gtrsim R_{\rm sph}$, for a subcritical disc, we have $\dot{M}_{\rm in} = \dot{M}$; otherwise, for a supercritical disc, then $\dot{M}_{\rm in} = \dot{M}(R_{\rm mag}/R_{\rm sph}) = \dot{M}_{\rm cr}$.

The model of Shakura & Sunyaev (1973) is based on the assumption of a standard geometrically thin disc. Most recently, Chashkina, Abolmasov & Poutanen (2017) proposed that the NS accretion disc could be geometrically thick and radiation pressure dominated in its inner part, leading to a larger magnetosphere size and, hence, a larger critical accretion rate of

$$\dot{M}_{\rm cr,1} \simeq 35\,\alpha_{-1}^{2/9}\mu_{30}^{4/9}\dot{M}_{\rm Edd}. \quad (5)$$

For a higher accretion rate, the inner disc would then become advection dominated and the critical rate can be further enhanced to (Chashkina et al. 2019)

$$\dot{M}_{\rm cr,2} \simeq 200\,\alpha_{-1}^{2/9}\mu_{30}^{4/9}\dot{M}_{\rm Edd}. \quad (6)$$

Therefore, one value of $\dot{M}_{\rm in}$ can be determined by two different magnetic field strengths. For example, for a $1.4\,{\rm M}_\odot$ NS with an accretion rate of $100\,\dot{M}_{\rm Edd}$, the magnetic field strength can be $\sim 5.6 \times 10^{12}$ G if the disc is radiation dominated by equation (5) or $\sim 1.1 \times 10^{11}$ G if the disc is advection dominated by equation (6), respectively. Here, $\alpha = 0.1$ and an NS radius of $R_{\rm NS} = 12.5$ km are adopted (e.g. Miller et al. 2019; Landry & Read 2021). Since we will discuss the influence of magnetic field decay on accretion rates in Section 3 and two different magnetic field strengths will give consistent results, for simplicity, we assume that the inner disc of the super-Eddington accretion disc during the Case BB/BC MT stage could always be advection dominated and, hence, we can use equation (6) to estimate critical accretion rate for specific NS magnetic field. The accretion rate of mgBHs formed after AICs of NSs is assumed to be limited by the Eddington limit, i.e. $\dot{M}_{\rm cr} = \dot{M}_{\rm Edd}$, because the magnetic field effect stops operating. The mass accretion rate of the compact object, including NS and BH, can be expressed as

$$\dot{M}_{\rm CO} = \begin{cases} (1-\eta)\dot{M} & \text{if } \dot{M} < \dot{M}_{\rm cr}, \\ (1-\eta)\dot{M}_{\rm cr}, & \text{if } \dot{M} > \dot{M}_{\rm cr}. \end{cases} \quad (7)$$

2.2 Physics implemented in MESA

We adopt the release version `mesa-r15140` of the Modules for Experiments in Stellar Astrophysics (MESA) stellar evolution code (Paxton et al. 2011, 2013, 2015, 2018, 2019; Jermyn et al. 2023) to evolve secondary He stars, which are assumed to be tidally locked by primary NS companions (treated as point masses). The zero-age He main-sequence stars are created following the same method with Qin et al. (2018, 2023), Bavera et al. (2020, 2021), Hu et al. (2022, 2023), Fragos et al. (2023), Lyu et al. (2023), Zhang et al. (2023), Wang et al. (2024), and then are relaxed to reach the thermal equilibrium. Convection is implemented based on the Ledoux criterion, and mixing-length theory (Böhm-Vitense 1958) with a mixing length of $\alpha_{\rm MLT} = 1.93$ is adopted. Convective mixing is treated as a top step decay process with an overshoot parameter $l_{\rm ov} = 0.1H_{\rm p}$, where $H_{\rm p}$ is the pressure scale height at the Ledoux boundary limit. We also consider semiconvection (Langer, Fricke & Sugimoto 1983) with an efficiency parameter $\alpha_{\rm SC} = 1.0$ in our model. The network of `approx12.net` is chosen for nucleosynthesis.

For stellar winds, we use the '`Dutch`' scheme for both `RGB` and `AGB` phase, as well as the cool and hot wind. We adopt the default `RGB_to_AGB_to_wind_switch = 1d-4`, as well as `cool_wind_full_on_T = 0.8d4` and `hot_wind_full_on_T = 1.2d4`. The standard '`Dutch`' scheme was calibrated by multiplying with a Dutch scaling factor of 0.667 to match the recently updated modelling of He star wind mass loss (Higgins et al. 2021) is adopted. Angular momentum transport and rotational mixing diffusive processes (Heger & Langer 2000; Heger, Langer & Woosley 2000), including the effects of Eddington–Sweet circulations, and the Goldreich–Schubert–Fricke instability, as well as secular and dynamical shear mixing, are incorporated. We adopt diffusive element mixing from these processes with an efficiency parameter of $f_{\rm c} = 1/30$ (Chaboyer & Zahn 1992; Heger & Langer 2000). Additionally, the traditional Spruit–Tayler (Spruit 2002) dynamo-induced angular momentum transport is implemented in our models.

We model MT following the Kolb scheme (Kolb & Ritter 1990), and the implicit MT method (Paxton et al. 2015) is adopted. The dynamical tides are applied to massive stars with radiative envelopes, and the corresponding time-scale for orbital synchronization is calculated following the prescription in Hurley, Tout & Pols (2002). We adopt the updated tidal torque coefficient E_2 provided in Qin et al. (2018).

3 PROPERTIES OF MGBH–NS FORMED THROUGH SUPER-EDDINGTON ACCRETION

We choose three different initial masses for the primary NS, including $M_{\rm 1,i}^{\rm NS} = 1.4$, 1.7, and $2.0\,{\rm M}_\odot$. If the primary NS mass exceeds $M_{\rm NS,max}$ during the process of super-Eddington accretion, the AIC to mgBH can occur. The initial He star mass $M_{\rm 2,i}^{\rm He}$ is in a range of 2.5–8 $\rm M_\odot$. We follow the evolution of these He stars from the zero-age He main sequence until carbon depletion occurred in their cores. Then, we estimate the baryonic mass of the remnant NS and BH formed through core collapse based on the delayed SN mechanism rather than the rapid SN mechanism (Fryer et al. 2012), prompted by recent plausible discoveries on compact objects in the lower mass gap (e.g. Thompson et al. 2019; Abbott et al. 2020b; Wyrzykowski & Mandel 2020). The baryonic mass of the remnant NS formed through electron-capture SN is set to $1.38\,{\rm M}_\odot$ following Fryer et al. (2012) if the pre-SN carbon–oxygen core mass is within the range between 1.37 and $1.43\,{\rm M}_\odot$ (Tauris, Langer & Podsiadlowski 2015). We also take into account neutrino loss as in Zevin et al. (2020). For the binary systems that could have MT, we cover the initial orbital periods $P_{\rm orb,i}$ of 0.04–40 d. Three critical super-Eddington accretion rates of $\dot{M}_{\rm cr} = 100\,\dot{M}_{\rm Edd}$, $300\,\dot{M}_{\rm Edd}$, and $500\,\dot{M}_{\rm Edd}$ are considered. For a $1.4\,{\rm M}_\odot$ NS, these three rates correspond to $\sim 3.6 \times 10^{-6}\,\kappa_{-0.47}^{-1}$, $\sim 1.1 \times 10^{-5}\,\kappa_{-0.47}^{-1}$, and $\sim 1.8 \times 10^{-5}\,\kappa_{-0.47}^{-1}\,{\rm M}_\odot\,{\rm yr}^{-1}$, which are always much lower than the MT rate of Case BB/BC (i.e. from a few 10^{-5} to a few $10^{-4}\,{\rm M}_\odot\,{\rm yr}^{-1}$; see Fig. 1). By setting $\alpha = 0.1$ and $R_{\rm NS} = 12.5$ km (e.g. Miller et al. 2019; Landry & Read 2021) in equation (6), NSs are required to have magnetic field of $\sim 1.1 \times 10^{11}$, $\sim 1.3 \times 10^{12}$, and $\sim 4.0 \times 10^{12}$ G, respectively. Besides defined parameters for evolving

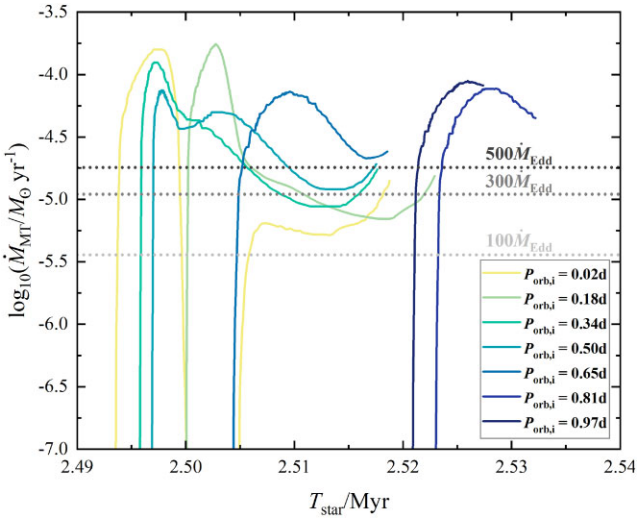

Figure 1. MT rate of binary systems as a function of the star age. We set an initial NS mass of $M_{1,i}^{NS} = 1.4\,M_\odot$, an initial He star mass of $M_{2,i}^{He} = 2.5\,M_\odot$, and $Z = Z_\odot$. Seven different initial orbital periods of $P_{orb,i} = 0.02,\ 0.18,\ 0.34,\ 0.50,\ 0.65,\ 0.81,$ and 0.97 d are considered. Three different super-Eddington accretion rates for a $1.4\,M_\odot$ NS, including $100\,\dot{M}_{Edd}$, $300\,\dot{M}_{Edd}$, and $500\,\dot{M}_{Edd}$, are marked with dashed lines.

binary systems introduced in Section 2.2, we set the grids of $M_{1,i}^{NS}$, $M_{2,i}^{He}$, $P_{orb,i}$, metallicity Z, and $\dot{M}_{cr}$ as initial input parameters to simulate the final primary mass $M_{1,f}$ and second-born NS/BH mass $M_{2,f}$ through MESA. When we consider the influence of accretion-induced magnetic field on the accreted mass and, hence, the final primary mass, we transfer the critical accretion rates to magnetic field strengths by equation (6) and evolve them with accreted masses.

We first ignore the possible decay of NS magnetic field and, hence, the accreting NSs can always have a constant critical super-Eddington accretion rate, since it is currently still unclear which physical effect, such as spin-down-induced flux expulsion, ohmic evolution of the crustal field, and diamagnetic screening of the field by accreted plasma, dominates the decay of magnetic field (e.g. Bhattacharya 2002). It is worth noting that the observation of a large bubble nebula surrounding NGC 1313 X-2 suggested that this ULX pulsar could have maintained a super-Eddington phase for more than 1 Myr, indicating that the magnetic field of this source has not been suppressed during the accreting phase (Sathyaprakash et al. 2019). Furthermore, despite the experience of extensive MT, some long-history accreting-powered pulsars could still have a strong magnetic field. For instance, the NS in low-mass X-ray binary 4U 1626−67 is almost older than 100 Myr, but its magnetic field is still as strong as a few 10^{12} G (Verbunt, Wijers & Burm 1990). Therefore, some NSs could accrete a large abundance of materials without losing their strong magnetic field.

Fig. 2 displays the parameter space that allows the formation of mgBH–NS binaries in a solar-metallicity environment, where $Z_\odot = 0.0142$ (Asplund et al. 2009) is employed in this work. We find that mgBH–NS binaries can hardly be formed via super-Eddington accretion from binary systems composed of $\lesssim 1.4\,M_\odot$ NSs and He stars. When the primary NSs with $M_{1,i}^{NS} \sim 1.7\,M_\odot$ have an accretion rate of $\gtrsim 300\,\dot{M}_{Edd}$ or the NSs with $M_{1,i}^{NS} \sim 2.0\,M_\odot$ have an accretion rate of $\sim 100\,\dot{M}_{Edd}$, AICs can happen only if the He star companions have an initial mass of $M_{2,i}^{He} \sim 3$–$5\,M_\odot$ and the binary systems have extremely close orbits with $P_{orb,i} \lesssim 0.2$ d. These AICs majorly occur duration the Case BB MT, and the second-born NSs could have a mass of $M_2^{NS} \sim 1.1$–$1.5\,M_\odot$ (see the left panel of Fig. 3). Furthermore, all NSs with a mass range of $\gtrsim 2.0\,M_\odot$ and an accretion rate of $\gtrsim 300\,\dot{M}_{Edd}$ that undergo the Case BB MT, as well as some undergoing the Case BC MT, can easily experience AIC to BHs. If the secondary is a $\sim 3\,M_\odot$ He star, the formation of mgBHs can be allowed for binary systems with an initial orbital period reaching $P_{orb,i} \sim 2$ d. In binary systems with $P_{orb,i} \lesssim 0.1$ d, the primary NSs can finally collapse, even if the secondary He stars are as massive as $M_{2,i}^{He} \sim 6\,M_\odot$. We note that the NS could undergo AIC if the initial binary system is composed of a $1.7\,M_\odot$ NS and a $2.5\,M_\odot$ He star that end up as a white dwarf (WD) with a critical accretion rate of $300\,\dot{M}_{Edd}$ (see the right-middle panel of Fig. 2), while AICs in the nearby MESA grid systems are prohibited, because the duration of the MT rate of this system above the rate is much longer compared to those of nearby MESA grid systems, as shown in Fig. 1.

Fig. 4 shows the allowed region for AICs of NSs at $Z = 0.1\,Z_\odot$. Usually, lower metallicity results in weaker wind mass loss of He stars and final carbon–oxygen cores with higher mass, so that the initial masses of He stars as a final fate of NS would be decreased overall, which is clearly shown in Fig. 3. He stars formed at lower metallicity environments also tend to be more compact and, hence, be more difficult to undergo MT, compared with equal-mass He stars at higher metallicity. In comparison to that at solar metallicity, Fig. 4 reveals that the subsolar metallicity AIC region for the same primary NS with a specific accretion rate moves toward a lower initial He star mass despite no significant change in the size of the region.

We now use an empirical formula from Osłowski et al. (2011), i.e.

$$B_{NS} = (B_{NS,0} - B_{NS,min}) \exp(-dM/\Delta M_d) + B_{NS,min}, \quad (8)$$

to consider possible accretion-induced magnetic field decay, where $B_{NS,0}$ is the initial magnetic field that is listed in Section 3 for different super-Eddington accretion rates, $B_{NS,min} = 10^8$ G is the minimal magnetic field of an NS, dM is the accreted mass, and $\Delta M_d = 0.05\,M_\odot$ given by Osłowski et al. (2011). By combining equation (6) and equation (8), we model the evolution of the NS magnetic field and accretion induced with the accreted mass in MESA. By setting three different initial critical accretion rates including $100\,\dot{M}_{Edd}$, $300\,\dot{M}_{Edd}$, and $500\,\dot{M}_{Edd}$, our simulated results at $Z = Z_\odot$ are displayed in Fig. 5. If we consider the possible accretion-induced magnetic field decay, Fig. 5 demonstrates that NSs are unlikely to accrete enough materials to become mgBHs if the initial mass of primary NS is $M_{1,i}^{NS} \lesssim 1.7\,M_\odot$ since the magnetic field strength and accretion rate decay rapidly with the increase of the NS mass. AICs can only be achievable when the primaries of binary NS–He star systems are high-mass NSs with $M_{1,i}^{NS} \gtrsim 2.0\,M_\odot$ and the accretion rates are $\gtrsim 300\,\dot{M}_{Edd}$. However, the AIC regions still reduce significantly relative to those without consideration of accretion-induced magnetic field decay. As shown in Fig. 5, these AICs occur in very close-orbit binary systems with low-mass He stars, which mainly undergo Case BB MT. Thus, if the magnetic field of NS could decay due to accretion, AICs could be hardly to happen via super-Eddington stable MT.

Accreting NSs during the Case BB/BC MT with super-Eddington accretion could form a population of mgBH–NS binaries. Because BHs formed after AICs of NSs could not continue to maintain super-Eddington accretions, the final masses of these mgBHs would be approach to or be a little higher than the Tolman–Oppenheimer–Vollkoff (TOV) mass of NS. Furthermore, this formation channel could generate amount of massive BNS systems, in which the primary NSs could have a mass that is close to the TOV mass of NS, if AICs do not happen during Case BB/BC MT. In Fig. 6, we show the post-

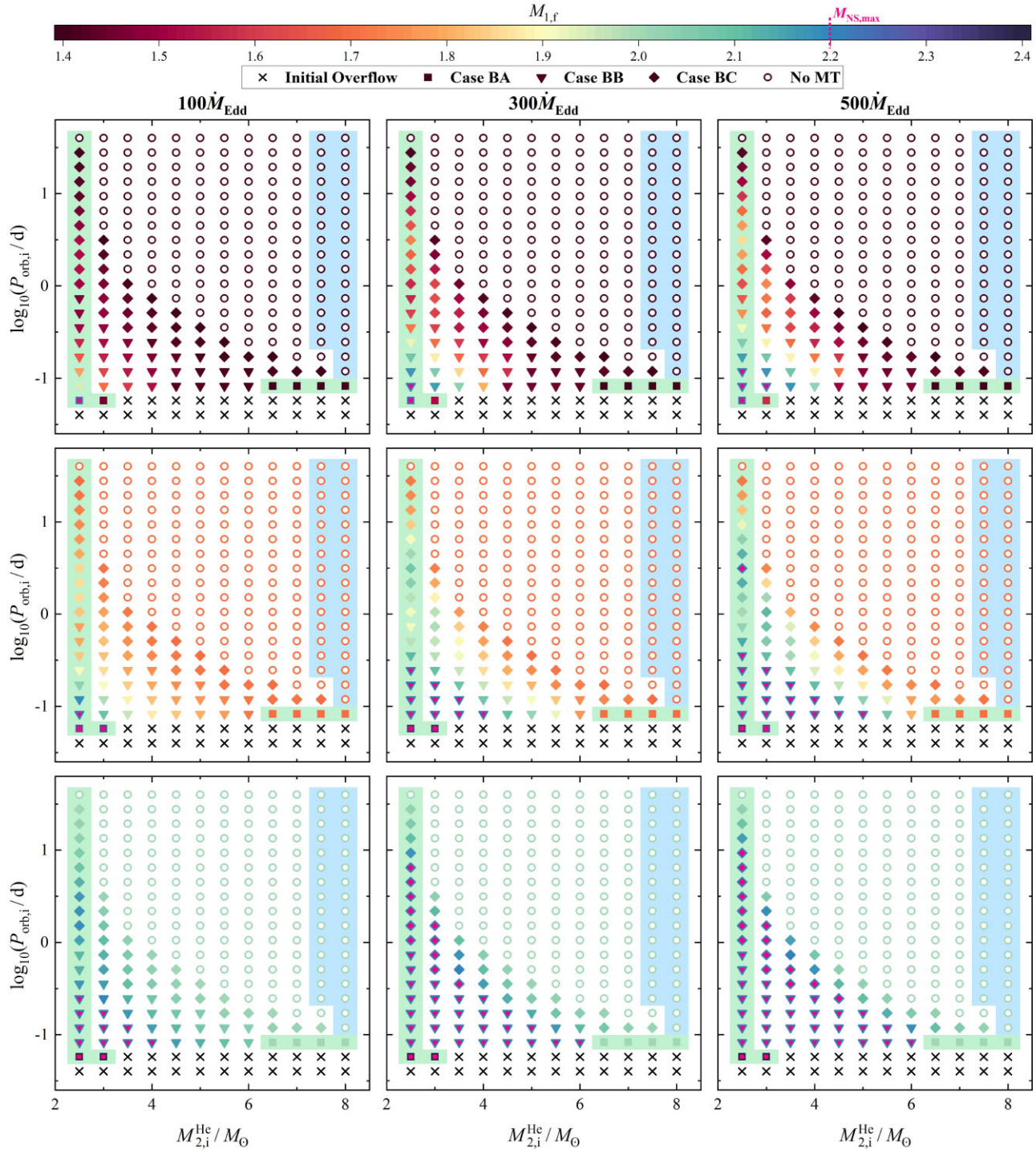

Figure 2. Final remnant mass (the colour bars) as a function of the initial mass of secondary He star $M_{2,i}^{He}$ and orbital period $P_{orb,i}$. Three different $M_{1,i}^{NS}$, including 1.4 $M_\odot$ (top panels), 1.7 $M_\odot$ (middle panels), and 2.0 $M_\odot$ (bottom panels) are considered. For each $M_{1,i}^{NS}$, we set three different critical accretion rates, i.e. 100 $\dot{M}_{Edd}$, 300 $\dot{M}_{Edd}$, and 500 $\dot{M}_{Edd}$ from left to right panels. Crosses, squares, triangles, diamonds, and circles represent the conditions of initial overflow, Case BA, Case BB, Case BC, and no MT, respectively. The points with pink interiors mark systems that can occur AIC of NS. Blue and green shading indicate where the He stars end up as WDs and BHs, respectively. We note that the colour bars are different for each $M_{1,i}^{NS}$.

MT separations of the evolved systems and then further estimate the inspiral time of the massive BNS and mgBH–NS systems. The SN kicks of our simulations are ignored, since most of the second SNe from the systems that undergo Case BB/BC MT would be ultrastripped SNe (Tauris et al. 2015). Our simplified simulations suggest that massive BNS and mgBH–NS systems that can merge within the Hubble time require an initial orbital period of $P_{orb,i} \lesssim$ 0.4–1 d. Tauris et al. (2017) and Hu et al. (2023) present that most of BNS and NSBH binaries would be survived after the second ultrastripped SNe due to weak kicks (see discussions in Tauris et al.

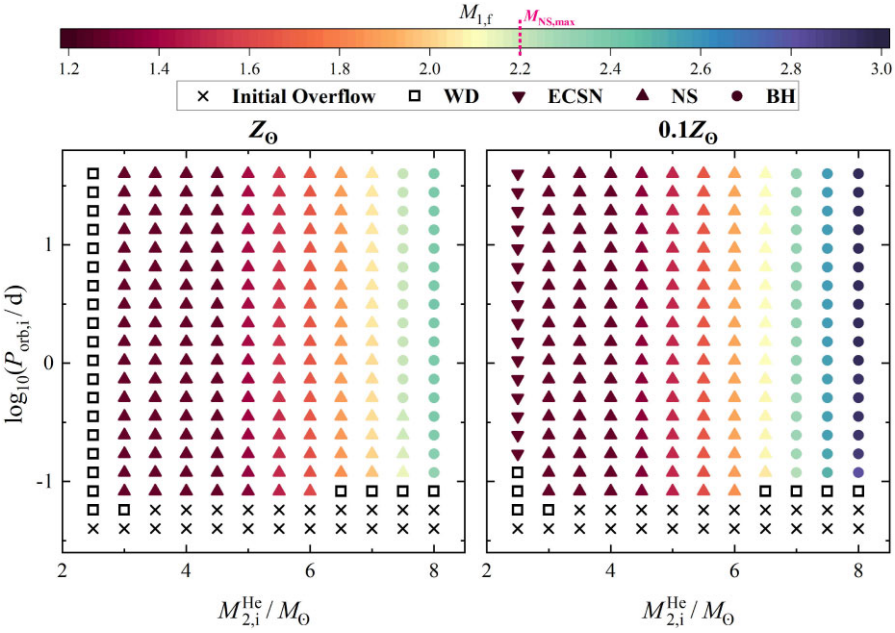

Figure 3. Mass of second-born NS and BH (the colour bars) as a function of the initial mass of secondary He star $M^{He}_{2,i}$ and initial orbital period $P_{orb,i}$. Left and right panels represent two different metallicities, i.e. $Z_\odot$ and $0.1\,Z_\odot$, respectively. Squares, lower triangles, upper triangles, and circles are the outcomes of WD, NS formed through electron-capture SN, NS formed through core-collapse SN, and BH. Since different initial primary NS masses and Eddington accretion limits have little impact on the mass of resulting compact objects, $M^{NS}_{1,i} = 1.4\,M_\odot$ and an accretion limit of 100 $\dot{M}_{Edd}$ are set here, while results by considering other different parameters limits are not shown. The maximum NS mass is set to $M_{NS,max} = 2.2\,M_\odot$.

2015) and can merge within the Hubble time if $P_{orb,i} \lesssim 0.4$ d, which is consistent with our simplified simulations in Fig. 6. Therefore, it is expected that these high-mass BNS and mgBH–NS binaries formed through super-Eddington stable MT are ideal GW sources in LIGO and *LISA* bands.

4 DISCUSSION

4.1 EM signatures

It has long been proposed that disrupted BH–NS mergers can power gamma-ray bursts (GRBs; e.g. Paczynski 1986, 1991; Eichler et al. 1989; Narayan, Paczynski & Piran 1992; Zhang 2018; Gottlieb et al. 2023) and kilonova emissions (e.g. Li & Paczyński 1998; Metzger et al. 2010; Kyutoku et al. 2015; Kawaguchi et al. 2016; Kasen et al. 2017; Barbieri et al. 2019; Zhu et al. 2020, 2022b; Darbha et al. 2021; Gompertz et al. 2023). Whether an NS can be tidally disrupted by the primary BH and eject a certain amount of material to generate EM counterparts could be described by the total amount of remnant mass $M_{total,fit}$ outside the BH horizon as a non-linear function of M_{BH}, the dimensionless projected aligned spin $\chi_{BH,z}$, M_{NS}, and R_{NS},[1] which has been given by an empirical model from Foucart, Hinderer & Nissanke (2018), i.e.

$$\frac{M_{total,fit}}{M^b_{NS}} = \left[\max\left(\alpha\frac{1-2C_{NS}}{\eta^{1/3}} - \beta\widetilde{R}_{ISCO}\frac{C_{NS}}{\eta} + \gamma, 0\right)\right]^\delta, \quad (9)$$

where M^b_{NS} is the NS baryonic mass, $C_{NS} = GM_{NS}/c^2R_{NS}$ is the compactness, $\widetilde{R}_{ISCO} = 3 + Z_2 - \mathrm{sign}(\chi_{BH,z})\sqrt{(3-Z_1)(3+Z_1+2Z_2)}$ is the normalized radius of the BH innermost stable circular orbit with $Z_1 = 1 + (1-\chi^2_{BH,z})^{1/3}[(1+\chi_{BH,z})^{1/3} + (1-\chi_{BH,z})^{1/3}]$ and $Z_2 = \sqrt{3\chi^2_{BH,z} + Z_1^2}$, $\eta = Q/(1+Q)^2$ in equation (9), and $Q = M_{BH}/M_{NS}$ is the mass ratio. The fitting parameters include $\alpha = 0.406$, $\beta = 0.139$, $\gamma = 0.255$, and $\delta = 1.761$. BH–NS mergers with system parameters falling into the parameter space where $M_{total,fit} = 0$ correspond to plunging events, while those with $M_{total,fit} > 0$ can allow tidal disruption to generate EM signals.

We adopt the AP4 model (Akmal & Pandharipande 1997) as the NS EoS, whose TOV mass is $M_{TOV} = 2.22\,M_\odot$ nearly consistent with $M_{NS,max}$ we used in Section 2. AP4 is one of the most likely EoSs allowed by the constraint on the observations of GW170817 (e.g. Abbott et al. 2018). We calculate M^b_{NS} as an empirical function of M_{NS} given by Gao et al. (2020), i.e. $M^b_{NS} = M_{NS} + A_1 \times M^2_{NS} + A_2 \times M^3_{NS}$, where $A_1 = 0.045$ and $A_2 = 0.023$, and M^b_{NS} and M_{NS} in this function are in units of $M_\odot$. $C_{NS} \approx 1.1056 \times (M^b_{NS}/M_{NS} - 1)^{0.8277}$ is estimated following the empirical formula constructed by Coughlin et al. (2017). In Fig. 7, we display the tidal disruption region for BH–NS mergers dependent on M_{BH}, $\chi_{BH,z}$, and M_{NS} by using equation (9).

For the standard isolated binary formation channel of BH–NS mergers, BH component unusually forms first in a wide orbit and, hence, could have a negligible spin since the tides are too weak to spin its progenitor up (see fig. 1 in Qin et al. 2018).[2] As shown in Fig. 7, if the mass gap is intrinsically existent, disrupted events

[1]NS spin can affect tidal disruption probability of BH–NS mergers. He stars can be efficiently spun up via tidal effects during the MT stage and finally remain fast-spinning NSs after SN explosions (Hu et al. 2023). However, these NSs can possess high magnetic field strengths, causing them to rapidly lose rotational energy through spin-down processes. Therefore, the spins of NSs during BH–NS mergers may always have little effect on tidal disruption.

[2]Under extreme conditions, the NS in a BH–NS binary could be born first due to a reversal in the mass ratio of progenitor stars during the Case A MT stage (Pols 1994; Broekgaarden et al. 2021; Román-Garza et al. 2021; Mould et al. 2022; Adamcewicz et al. 2024). The BH progenitors can thus be tidally

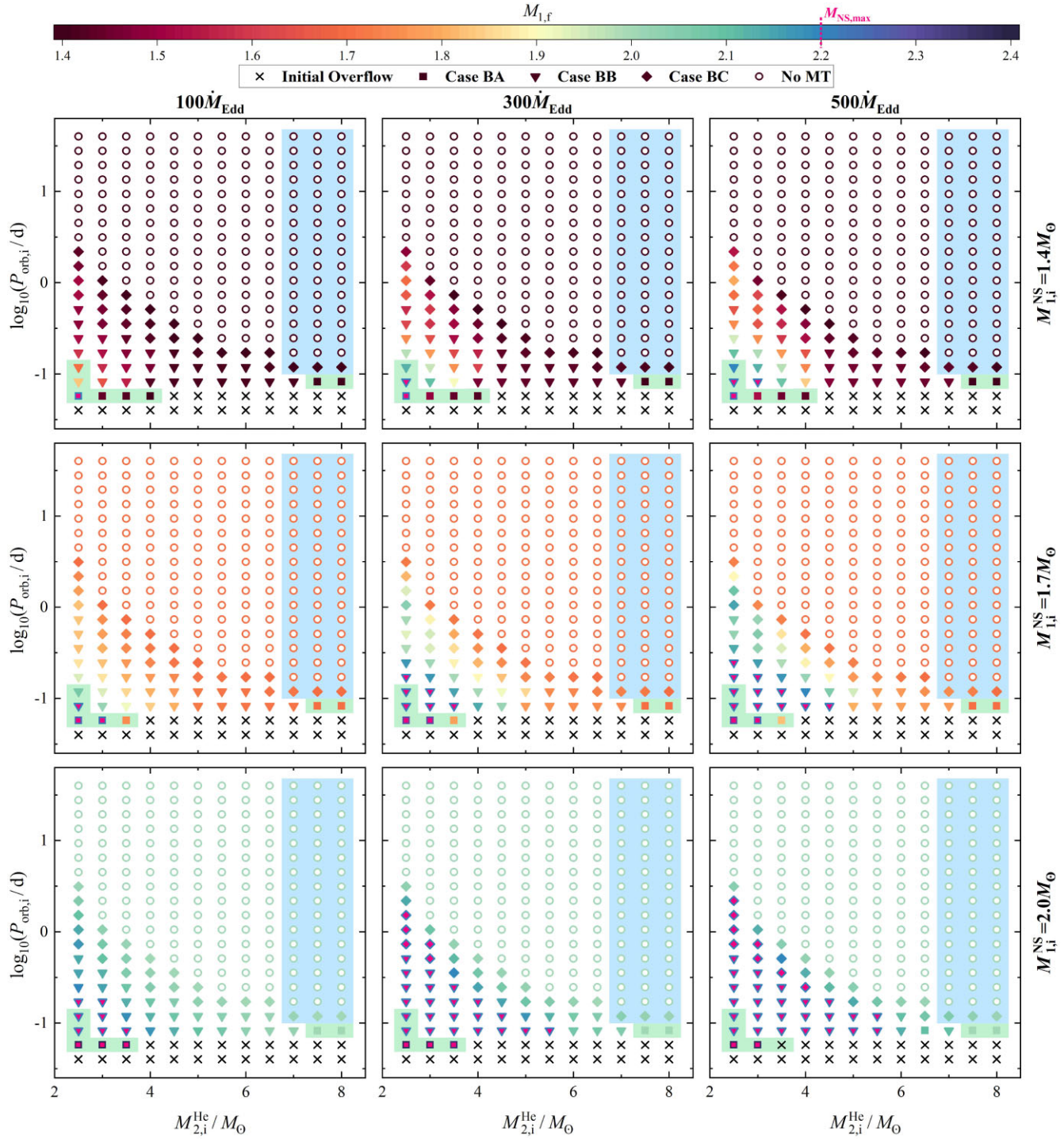

Figure 4. Similar to Fig. 2, but for $Z = 0.1\,Z_\odot$.

could only contribute a limited fraction of BH–NS population in the universe, which would require a mass space of $M_{BH} \lesssim 6\,M_\odot$ and $M_{NS} \lesssim 1.2\,M_\odot$. For example, GW200105 (GW200115) reported by the LVK Collaboration in O3 (Abbott et al. 2021b) is formed through a merger between a $8.9^{+1.1}_{-1.3}\,M_\odot$ ($5.9^{+1.4}_{-2.1}\,M_\odot$) BH with a dimensionless projected aligned spin of $-0.01^{+0.10}_{-0.16}$ ($-0.18^{+0.21}_{-0.57}$) and a $1.9^{+0.2}_{-0.2}\,M_\odot$ ($1.4^{+0.6}_{-0.2}\,M_\odot$) NS, inferred from low-spin priors of the secondary. Mandel & Smith (2021) found that GW200115 could be more constrained, with $M_{BH} = 7.0^{+0.4}_{-0.4}\,M_\odot$ and $M_{NS} = 1.25^{+0.09}_{-0.09}\,M_\odot$, by adopting a zero-spin prior preference. Thus, these two BH–NS mergers could possess BH components with mass above the mass gap, and their formation channels could align with the standard picture (e.g. Broekgaarden & Berger 2021; Chattopadhyay et al. 2022; Zhu et al. 2022a; Jiang et al. 2023). Apparently, Fig. 7 suggested that these mergers could hardly make tidal disruption

spun up after the common-envelope stage, finally remaining fast-spinning BHs (Hu et al. 2022).

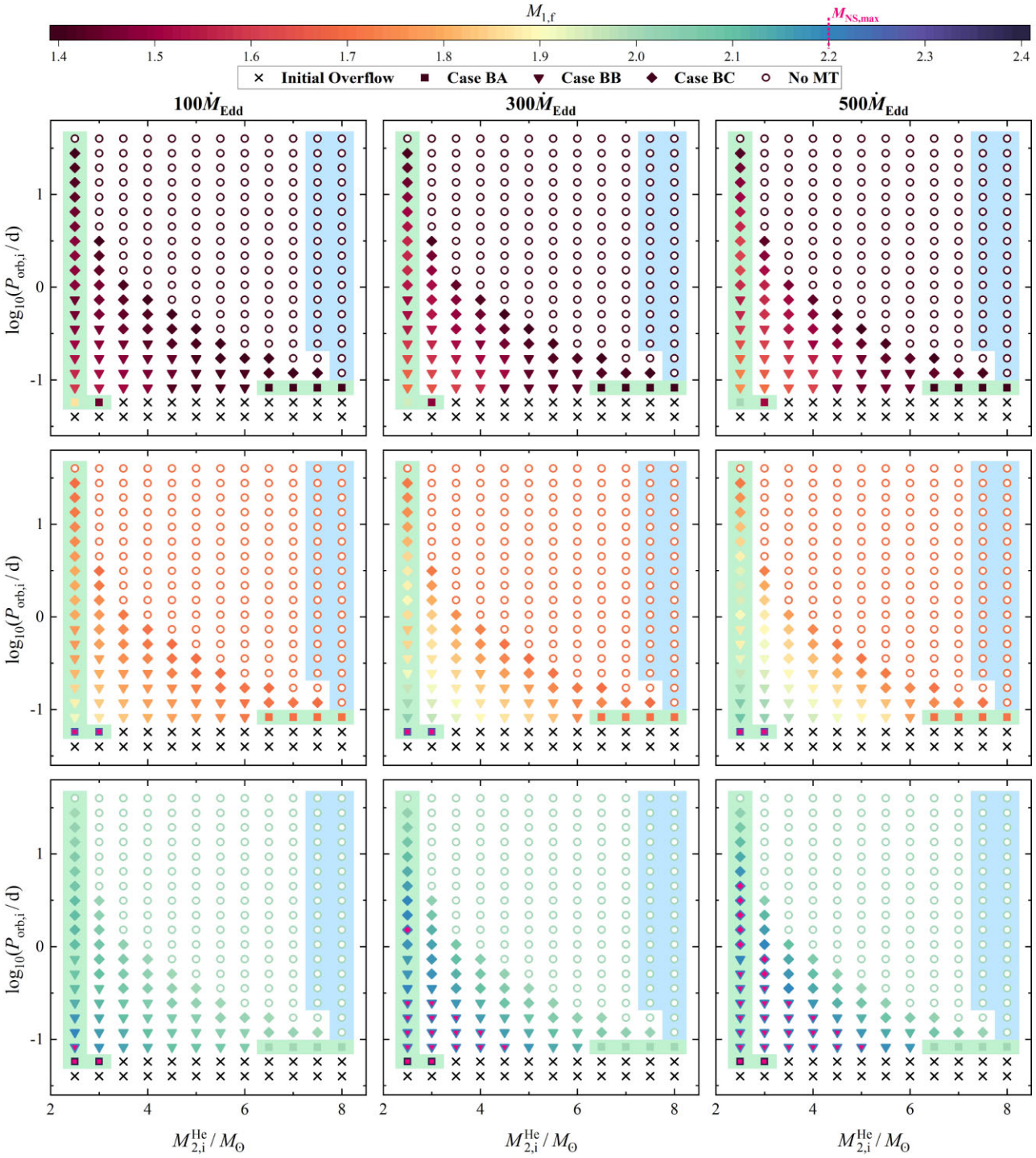

Figure 5. Similar to Fig. 2, but consider the accretion-induced magnetic field decay of NS.

to generate EM counterparts, consistent with the conclusion from Fragione (2021), Zhu et al. (2021), D'Orazio et al. (2022), Gompertz et al. (2022), and Biscoveanu et al. (2023). In contrast, mgBHs could be more likely to tidally disrupt more massive NSs. Fig. 7 shows that mergers between zero-spin mgBHs and NSs can easily undergo tidal disruption as long as $M_{NS} \lesssim 1.2$–$1.5\,M_\odot$.

Our detailed binary simulations shown in Section 3 suggest that mgBHs formed via super-Eddington accretion during the Case BB/BC MT could have a mass nearly equal to or slightly higher than $M_{NS,max}$. Unless the mass of secondaries is $\gtrsim 1.5\,M_\odot$, tidal disruption can always happen. As an example in Fig. 7, we show all our MESA grid data capable of forming mgBH–NS mergers at a metallicity of $Z_\odot$ in Fig. 2. Although only four data points of mgBH–NS mergers are visible in Fig. 7, we note that actually a total of 82 data points are included, as they are overlapping. One can find that the secondaries for those binary systems that experience Case BB/BC could mostly have a mass of $\lesssim 1.5\,M_\odot$, which are located in the parameter region that allows tidal disruption. Thus, it is expected that a large proportion

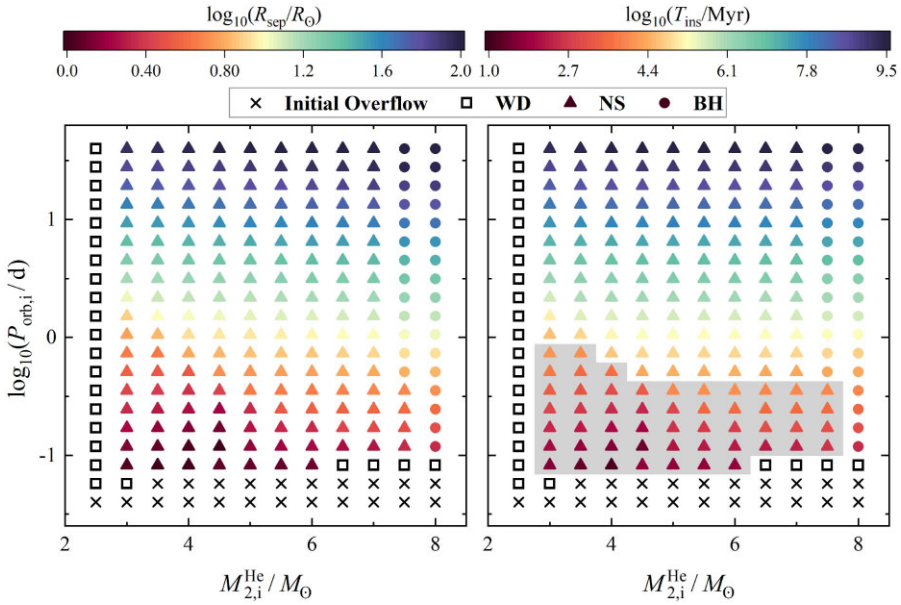

Figure 6. The left panel corresponds to the post-MT separation at the pre-SN stage and the right one refers to the inspiral time of the massive BNS and mgBH–NS systems, respectively. The light grey region marks the parameter space in which the compact object binaries can merge within the Hubble time. Since different initial primary NS masses and Eddington accretion limits have little impact on post-MT separations and inspiral times, $M_{1,i}^{NS} = 1.4\,M_\odot$ and an accretion limit of 100 $\dot{M}_{Edd}$ are set here, while results by considering other different parameters limits are not shown.

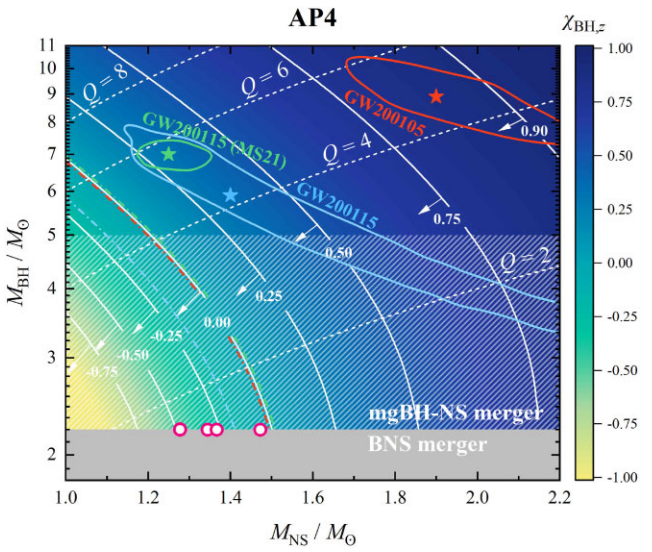

Figure 7. The source-frame mass parameter space for BH–NS merger systems to allow tidal disruption of the NS by the BH with consideration of the AP4 EoS model. The dashed lines represent the mass ratio from $Q = 2$ to 8. We mark several values of the primary BH spin along the orbital angular momentum from $\chi_{BH,z} = -0.75$ to 0.90 as solid lines. For a specific $\chi_{BH,z}$, the BH–NS mergers with component masses located at the bottom left parameter space (denoted by the direction of the arrows) can have $M_{tot,fit} > 0$, indicating that these mergers can allow tidal disruption. The grey and white shadow regions represent that the mass of the primary compact objects falls below the NS maximum mass and into the mass gap, respectively. The binary systems that can form mgBH–NS mergers, as shown in Fig. 2, are marked as pink empty points. The 90 per cent credible posterior distributions (coloured solid lines) and the medians (coloured stars) of GW200105 (orange), GW200115 (blue; Abbott et al. 2021b), and GW200115 (green) obtained by applying an astrophysically motivated priors (Mandel & Smith 2021) are displayed, while corresponding median values of $\chi_{BH,z}$ for these two sources are marked as dashed–dotted lines.

of mgBH–NS mergers formed through super-Eddington stable MT would undergo tidal disruption to generate EM signals.

4.2 Constraints on the NS TOV mass and EoS

In Section 3, we suggest that binary systems undergoing super-Eddington stable MT can finally generate a population of GW NS binaries, comprising either an NS with a mass close to M_{TOV} or an mgBH with a mass slightly higher than M_{TOV}. Distinguishing between these high-mass BNS and mgBH–NS mergers using GW and EM observations can help constrain the NS TOV mass and EoS.

In the case of an mgBH–NS merger, GW emissions would abruptly terminate upon the tidal disruption of the NS, without exciting quasi-normal modes (Shibata et al. 2009). However, for a massive BNS involving an M_{TOV} NS, the outcome of the merger is a prompt collapse accompanied with ringdown emission from the remnant BH. The difference of GW merger phase in the kilohertz range between these scenarios could be discerned with the advent of third-generation detectors (e.g. Shibata et al. 2009; Kyutoku et al. 2020).

Despite prompt collapse after merging, a typical-mass NS in an asymmetric BNS system with a companion of an M_{TOV} NS can be tidally disrupted to power a bright kilonova signal. These asymmetric BNS mergers can generate disc outflow and massive lanthanide-rich dynamical ejecta, whose kilonovae are similar to those from mergers between $\gtrsim 5\,M_\odot$ BH and NS (e.g. Sekiguchi et al. 2016; Bernuzzi et al. 2020). However, numerical relativity simulations revealed that the mass of dynamical ejecta from mgBH–NS mergers could be lower by an order of magnitude compared to that from corresponding BNS binaries, or even negligible (Foucart et al. 2019; Kyutoku et al. 2020; Hayashi et al. 2021). Thus, the kilonova emissions from low-mass mgBH–NS mergers could lack the contribution from lanthanide-rich dynamical ejecta, which can be used to distinguish mgBH–NS mergers from high-mass BNS mergers through follow-up observations.

Thus, we expect that NS–He star binaries with super-Eddington stable MT could serve as a plausible formation channel to form a population of high-mass BNS and low-mass mgBH–NS GWs. Future GW and EM observations on a large number of these NS binaries could provide a precise mass boundary between NSs and BHs.

5 CONCLUSIONS

In this paper, we propose a new scenario for the formation of mgBH–NS binaries. A fraction of NSs with companions of He stars could have super-Eddington stable MT, as suggested by both observations and theory. We evolve NS–He star binaries by our detailed binary simulations to explore the parameter space that allows for the AICs of NSs. Since super-Eddington accretion can be maintained during the Case BB/BC MT stage, our simulated results reveal that AIC events tend to happen when the primary NSs have an initial mass $\gtrsim 1.7\,M_\odot$ with an accretion rate of $\gtrsim 300\,\dot{M}_{\rm Edd}$. This formation scenario can thus generate a population of NS binaries consisting of an mgBH with a mass slightly higher than $M_{\rm TOV}$ for AIC events or an NS with a mass close to $M_{\rm TOV}$ if AICs do not happen, which can eventually merge within the Hubble time to become ideal GW sources. However, it is difficult to evaluate how common such a scenario is for forming mgBH–NS mergers based on our present knowledge. On the one hand, low-mass NSs are more common than high-mass NSs inferred by the Galactic pulsar observations (Lattimer 2012; Antoniadis et al. 2016; Alsing et al. 2018; Farr & Chatziioannou 2020) and population synthesis simulations (e.g. Giacobbo & Mapelli 2018; Vigna-Gómez et al. 2018; Broekgaarden et al. 2022). The lack of high-mass primary NSs in BNS systems makes it difficult for AICs to happen. On the other hand, GW190425 was measured to have a heavy primary NS with a mass of $\sim$1.61–2.52 $M_\odot$ (Abbott et al. 2020a), accompanied by an unexpectedly high event rate density, if it had a BNS origin. Furthermore, the NSs observed in BNS and BH–NS mergers detected via GWs exhibit a uniform distribution in mass (Landry & Read 2021; Zhu et al. 2022a; Abbott et al. 2023a

), contrary to the Galactic pulsar observations and population synthesis simulations. Systems between high-mass NSs and He stars may be widespread in the universe, suggesting that AICs via super-Eddington stable MT are not necessarily impossible.

These mgBH–NS mergers can easily lead to tidal disruption, generating bright EM signals. Future GW and EM observations on the population of these NS binaries formed via super-Eddington stable MT could help us constrain the TOV mass and EoS of NSs.

ACKNOWLEDGEMENTS

J-PZ thanks Team COMPAS group for useful discussions. This work was supported by Anhui Provincial Natural Science Foundation (grant no. 2308085MA29) and the Natural Science Foundation of Universities in Anhui Province (grant no. KJ2021A0106).

DATA AVAILABILITY

The data generated in this work will be shared upon reasonable request to the corresponding author.

REFERENCES

Abbott B. P. et al., 2018, Phys. Rev. Lett., 121, 161101
Abbott B. P. et al., 2020a, ApJ, 892, L3
Abbott R. et al., 2020b, ApJ, 896, L44
Abbott R. et al., 2021a, Phys. Rev. X, 11, 021053
Abbott R. et al., 2021b, ApJ, 915, L5
Abbott R. et al., 2023a, Phys. Rev. X, 13, 011048
Abbott R. et al., 2023b, Phys. Rev. X, 13, 041039
Adamcewicz C., Galaudage S., Lasky P. D., Thrane E., 2024, ApJ, 964, L6
Akmal A., Pandharipande V. R., 1997, Phys. Rev. C, 56, 2261
Alsing J., Silva H. O., Berti E., 2018, MNRAS, 478, 1377
Andrews J. J., Taggart K., Foley R., 2022, preprint (arXiv:2207.00680)
Antoniadis J. et al., 2013, Science, 340, 448
Antoniadis J., Tauris T. M., Ozel F., Barr E., Champion D. J., Freire P. C. C., 2016, preprint (arXiv:1605.01665)
Asplund M., Grevesse N., Sauval A. J., Scott P., 2009, ARA&A, 47, 481
Bachetti M. et al., 2014, Nature, 514, 202
Bailyn C. D., Jain R. K., Coppi P., Orosz J. A., 1998, ApJ, 499, 367
Barbieri C., Salafia O. S., Perego A., Colpi M., Ghirlanda G., 2019, A&A, 625, A152
Bavera S. S. et al., 2020, A&A, 635, A97
Bavera S. S. et al., 2021, A&A, 647, A153
Belczynski K., Wiktorowicz G., Fryer C. L., Holz D. E., Kalogera V., 2012, ApJ, 757, 91
Belczynski K., Done C., Hagen S., Lasota J.-P., Sen K., 2021, preprint (arXiv:2111.09401)
Bernuzzi S. et al., 2020, MNRAS, 497, 1488
Bhattacharya D., 2002, J. Astrophys. Astron., 23, 67
Bhattacharya D., van den Heuvel E. P. J., 1991, Phys. Rep., 203, 1
Biscoveanu S., Landry P., Vitale S., 2023, MNRAS, 518, 5298
Böhm-Vitense E., 1958, Z. Astrophys., 46, 108
Broekgaarden F. S., Berger E., 2021, ApJ, 920, L13
Broekgaarden F. S. et al., 2021, MNRAS, 508, 5028
Broekgaarden F. S. et al., 2022, MNRAS, 516, 5737
Chaboyer B., Zahn J. P., 1992, A&A, 253, 173
Chashkina A., Abolmasov P., Poutanen J., 2017, MNRAS, 470, 2799
Chashkina A., Lipunova G., Abolmasov P., Poutanen J., 2019, A&A, 626, A18
Chattopadhyay D., Stevenson S., Broekgaarden F., Antonini F., Belczynski K., 2022, MNRAS, 513, 5780
Chen H.-L., Tauris T. M., Chen X., Han Z., 2023, ApJ, 951, 91
Coughlin M., Dietrich T., Kawaguchi K., Smartt S., Stubbs C., Ujevic M., 2017, ApJ, 849, 12
Darbha S., Kasen D., Foucart F., Price D. J., 2021, ApJ, 915, 69
Dermer C. D., Atoyan A., 2006, ApJ, 643, L13
D'Orazio D. J., Haiman Z., Levin J., Samsing J., Vigna-Gómez A., 2022, ApJ, 927, 56
Drozda P., Belczynski K., O'Shaughnessy R., Bulik T., Fryer C. L., 2022, A&A, 667, A126
Eichler D., Livio M., Piran T., Schramm D. N., 1989, Nature, 340, 126
Esteban I., Beacom J. F., Kopp J., 2023, preprint (arXiv:2310.19868)
Farah A., Fishbach M., Essick R., Holz D. E., Galaudage S., 2022, ApJ, 931, 108
Farr W. M., Chatziioannou K., 2020, Res. Notes Am. Astron. Soc., 4, 65
Farr W. M., Sravan N., Cantrell A., Kreidberg L., Bailyn C. D., Mandel I., Kalogera V., 2011, ApJ, 741, 103
Fishbach M., Kalogera V., 2022, ApJ, 929, L26
Foucart F., Hinderer T., Nissanke S., 2018, Phys. Rev. D, 98, 081501
Foucart F., Duez M. D., Kidder L. E., Nissanke S. M., Pfeiffer H. P., Scheel M. A., 2019, Phys. Rev. D, 99, 103025
Fragione G., 2021, ApJ, 923, L2
Fragos T. et al., 2023, ApJS, 264, 45
Frank J., King A., Raine D. J., 2002, Accretion Power in Astrophysics, 3rd edn. Cambridge Univ. Press, Cambridge
Fryer C. L., Belczynski K., Wiktorowicz G., Dominik M., Kalogera V., Holz D. E., 2012, ApJ, 749, 91
Fürst F. et al., 2016, ApJ, 831, L14
Gao H., Ai S.-K., Cao Z.-J., Zhang B., Zhu Z.-Y., Li A., Zhang N.-B., Bauswein A., 2020, Front. Phys., 15, 24603
Gao S.-J., Li X.-D., Shao Y., 2022, MNRAS, 514, 1054
Ghosh P., Lamb F. K., 1979, ApJ, 234, 296
Giacobbo N., Mapelli M., 2018, MNRAS, 480, 2011

Giacomazzo B., Perna R., 2012, ApJ, 758, L8
Gompertz B. P., Nicholl M., Schmidt P., Pratten G., Vecchio A., 2022, MNRAS, 511, 1454
Gompertz B. P., Nicholl M., Smith J. C., Harisankar S., Pratten G., Schmidt P., Smith G. P., 2023, MNRAS, 526, 4585
Gottlieb O. et al., 2023, ApJ, 954, L21
Hayashi K., Kawaguchi K., Kiuchi K., Kyutoku K., Shibata M., 2021, Phys. Rev. D, 103, 043007
Heger A., Langer N., 2000, ApJ, 544, 1016
Heger A., Langer N., Woosley S. E., 2000, ApJ, 528, 368
Higgins E. R., Sander A. A. C., Vink J. S., Hirschi R., 2021, MNRAS, 505, 4874
Hu R.-C., Zhu J.-P., Qin Y., Zhang B., Liang E.-W., Shao Y., 2022, ApJ, 928, 163
Hu R.-C. et al., 2023, preprint (arXiv:2301.06402)
Hurley J. R., Tout C. A., Pols O. R., 2002, MNRAS, 329, 897
Israel G. L. et al., 2017, Science, 355, 817
Jermyn A. S. et al., 2023, ApJS, 265, 15
Jiang L., Chen W.-C., Tauris T. M., Müller B., Li X.-D., 2023, ApJ, 945, 90
Kaaret P., Feng H., Roberts T. P., 2017, ARA&A, 55, 303
Kasen D., Metzger B., Barnes J., Quataert E., Ramirez-Ruiz E., 2017, Nature, 551, 80
Kawaguchi K., Kyutoku K., Shibata M., Tanaka M., 2016, ApJ, 825, 52
Kolb U., Ritter H., 1990, A&A, 236, 385
Kreidberg L., Bailyn C. D., Farr W. M., Kalogera V., 2012, ApJ, 757, 36
Kulkarni A. K., Romanova M. M., 2013, MNRAS, 433, 3048
Kyutoku K., Ioka K., Okawa H., Shibata M., Taniguchi K., 2015, Phys. Rev. D, 92, 044028
Kyutoku K., Fujibayashi S., Hayashi K., Kawaguchi K., Kiuchi K., Shibata M., Tanaka M., 2020, ApJ, 890, L4
Landry P., Read J. S., 2021, ApJ, 921, L25
Langer N., Fricke K. J., Sugimoto D., 1983, A&A, 126, 207
Lattimer J. M., 2012, Annu. Rev. Nucl. Part. Sci., 62, 485
Li L.-X., Paczyński B., 1998, ApJ, 507, L59
Long M., Romanova M. M., Lovelace R. V. E., 2005, ApJ, 634, 1214
Lyu F. et al., 2023, MNRAS, 525, 4321
MacFadyen A. I., Ramirez-Ruiz E., Zhang W., 2005, preprint (arXiv:astro-ph/0510192)
MacLeod M., Ramirez-Ruiz E., 2015, ApJ, 798, L19
Mandel I., Müller B., 2020, MNRAS, 499, 3214
Mandel I., Smith R. J. E., 2021, ApJ, 922, L14
Mandel I., Müller B., Riley J., de Mink S. E., Vigna-Gómez A., Chattopadhyay D., 2021, MNRAS, 500, 1380
Margalit B., Metzger B. D., 2017, ApJ, 850, L19
Metzger B. D. et al., 2010, MNRAS, 406, 2650
Miller M. C. et al., 2019, ApJ, 887, L24
Mould M., Gerosa D., Broekgaarden F. S., Steinle N., 2022, MNRAS, 517, 2738
Narayan R., Paczynski B., Piran T., 1992, ApJ, 395, L83
Olejak A., Fryer C. L., Belczynski K., Baibhav V., 2022, MNRAS, 516, 2252
Osłowski S., Bulik T., Gondek-Rosińska D., Belczyński K., 2011, MNRAS, 413, 461
Özel F., Psaltis D., Narayan R., McClintock J. E., 2010, ApJ, 725, 1918
Paczynski B., 1986, ApJ, 308, L43
Paczynski B., 1991, Acta Astron., 41, 257
Paxton B., Bildsten L., Dotter A., Herwig F., Lesaffre P., Timmes F., 2011, ApJS, 192, 3
Paxton B. et al., 2013, ApJS, 208, 4
Paxton B. et al., 2015, ApJS, 220, 15
Paxton B. et al., 2018, ApJS, 234, 34
Paxton B. et al., 2019, ApJS, 243, 10
Podsiadlowski P., Rappaport S., Han Z., 2003, MNRAS, 341, 385
Pols O. R., 1994, A&A, 290, 119
Qin Y., Fragos T., Meynet G., Andrews J., Sørensen M., Song H. F., 2018, A&A, 616, A28
Qin Y., Hu R. C., Meynet G., Wang Y. Z., Zhu J. P., Song H. F., Shu X. W., Wu S. C., 2023, A&A, 671, A62
Rivinius T., Baade D., Hadrava P., Heida M., Klement R., 2020, A&A, 637, L3
Román-Garza J. et al., 2021, ApJ, 912, L23
Romani R. W., Kandel D., Filippenko A. V., Brink T. G., Zheng W., 2022, ApJ, 934, L17
Sathyaprakash R. et al., 2019, MNRAS, 488, L35
Sekiguchi Y., Kiuchi K., Kyutoku K., Shibata M., Taniguchi K., 2016, Phys. Rev. D, 93, 124046
Shakura N. I., Sunyaev R. A., 1973, A&A, 24, 337
Shao Y., Li X.-D., 2021, ApJ, 920, 81
Shao Y., Li X.-D., Dai Z.-G., 2019, ApJ, 886, 118
Shibata M., Kyutoku K., Yamamoto T., Taniguchi K., 2009, Phys. Rev. D, 79, 044030
Spruit H. C., 2002, A&A, 381, 923
Tauris T. M., Langer N., Podsiadlowski P., 2015, MNRAS, 451, 2123
Tauris T. M. et al., 2017, ApJ, 846, 170
Thompson T. A. et al., 2019, Science, 366, 637
van der Meij V., Guo D., Kaper L., Renzo M., 2021, A&A, 655, A31
van Son L. A. C. et al., 2022, ApJ, 940, 184
Verbunt F., Wijers R. A. M. J., Burm H. M. G., 1990, A&A, 234, 195
Vigna-Gómez A. et al., 2018, MNRAS, 481, 4009
Wang Y. M., 1996, ApJ, 465, L111
Wang Z.-H.-T. et al., 2024, preprint (arXiv:2401.17558)
Wyrzykowski Ł., Mandel I., 2020, A&A, 636, A20
Xing Z. et al., 2023, preprint (arXiv:2309.09600)
Ye C., Fishbach M., 2022, ApJ, 937, 73
Zevin M., Spera M., Berry C. P. L., Kalogera V., 2020, ApJ, 899, L1
Zhang B., 2018, The Physics of Gamma-Ray Bursts. Cambridge Univ. Press, Cambridge
Zhang W. T. et al., 2023, MNRAS, 526, 854
Zhou C., Feng H., Bian F., 2023, ApJ, 947, 52
Zhu J.-P., Yang Y.-P., Liu L.-D., Huang Y., Zhang B., Li Z., Yu Y.-W., Gao H., 2020, ApJ, 897, 20
Zhu J.-P., Wu S., Yang Y.-P., Zhang B., Yu Y.-W., Gao H., Cao Z., Liu L.-D., 2021, ApJ, 921, 156
Zhu J.-P., Wu S., Qin Y., Zhang B., Gao H., Cao Z., 2022a, ApJ, 928, 167
Zhu J.-P., Wang X. I., Sun H., Yang Y.-P., Li Z., Hu R.-C., Qin Y., Wu S., 2022b, ApJ, 936, L10

This paper has been typeset from a TEX/LATEX file prepared by the author.